Journal of Scientific & Industrial Research
Vol. 81, August 2022, pp. 882-892
10.56042/jsir.v81i08.53806

Parameters Influencing the Performance of a Single Needle to Plane EHD Drying Mechanism

Mohammad Saifullah Khan* & Minhaj Ahemad

Department of Mechanical Engineering, St. Vincent Pallotti College of Engineering & Technology, Nagpur 441 108, Maharashtra, India

Received 13 August 2021; revised 23 July 2022; accepted 23 July 2022

Electrohydrodynamics (EHD) has found prominence in several studies due to its utilization of a low power consuming corona discharge for achieving the drying enhancement. Corona discharge forms the core functionality of Electrohydrodynamics (EHD) drying, which deals with the performance enhancement of an application by controlling the corona discharge or ionic wind. A phenomenon known as the corona discharge is induced, when the electric field around a charged conductor is strong enough to ionize the surrounding dielectric gas molecules but not strong enough to cause an electrical breakdown. This discharge assists in mass transfer enhancement. Controlled corona discharge can be used in drying enhancement, and similar applications. These applications are energy-efficient, cost-effective, cleaner, and greener processes, with a non-mechanical design that allows rapid control over the drying. This gives EHD drying an advantage over conventional drying processes. In this review, an effort has been made to summarize various performance parameters associated with needle-to-plane configuration-based EHD drying mechanisms which can help in development of an effective configuration to build a large scale industrial drying setup.

Keywords: Electrohydrodynamics, Corona discharge, EHD drying, Ionic wind

Introduction

Drying is integral to several industrial processes, wherein it is achieved by various means. Most of these techniques involve significant thermal variation for the removal of moisture, which can have a significant effect on physicochemical properties[1], overall quality[2], appearance[3], and microstructural characteristics of the product. Moreover, these techniques consume high energy in achieving the desired outcome.[4] A process like freeze-drying[5], oven drying[4], auxiliary heating[6], and osmotic dewatering (drying)[7] are energy-intensive processes, which leave by-products, effluents, and greenhouse gases as part of the process, that can adversely affect the environment. Energy losses associated with these processes are also high. A separate treatment plant needs to be set up to treat the by-products, effluents, and greenhouse gases, which adds to both the economic and energy aspect of the process. Hence, the Industry needs an economical and energy-efficient process, which would result in efficient drying along with a minimal impact on both product quality and the environment.

Electrohydrodynamics (EHD) enhanced drying has stood out as a greener alternative to conventional industrial drying techniques due to its non-thermal drying enhancement ability[8], which can be achieved at very low energy consumption.[9] Another advantage of EHD is its non-mechanical design, which prevents it from any mechanical failures. These aspects have led to extensive research over the past several decades to come up with an EHD-based delivery system for commercial drying applications. Hence, there is a need to further research EHD to develop a mechanism to address large-scale drying that could replace the conventional industrial drying techniques.

One of the core aspects of EHD is the electrode configuration that is used to achieve the desired outcome. EHD makes use of several types of electrode configurations, which are the combinations of the emitting and collecting/ground electrodes. Various application-specific electrode configurations have been experimented with over the years to utilize the benefits of the corona discharge (ionic wind). Some of the most prominent configurations that were experimented with, in the recent past are 'needle to plane[10]', 'wire to plane[11]', 'wire to cylinder[12]', 'needle to ring[13]', and other configurations. The preliminary research work in the field of Electrohydrodynamics (EHD) was focused on point (needle) to plane configuration[10] and the concept of corona discharge (ionic wind).

*Author for Correspondence
E-mail: skhan@stvincentngp.edu.in

The needle-to-plane EHD mechanism is one of the most versatile electrode configurations for the enhancement of drying, but to date, a large-scale industrial model has not been developed.[14] Hence, the focus of the current review is to study the performance parameters associated with corona discharge in needle-to-plane EHD drying applications. And to narrow down the performance parameters, which would help in coming up with the optimum values of parameters like applied polarity, electrode gap (d), electrode spacing (S), cross-flow (u), and other geometric parameters, that could lead to the development of an effective configuration of a needle-to-plane based EHD drying model for a possible industrial application.

Electrohydrodynamics (EHD) and the Drying Process

Electrohydrodynamics (Electro-Hydro-Dynamics or EHD) is the phenomenon that involves the direct conversion of electrical energy into kinetic energy, and it deals with fluid motion induced by the electric field.[15]

The 'Needle-to-plane' electrohydrodynamic (EHD) drying mechanism, shown in Fig. 1, consists of a sharply pointed needle electrode perpendicular (axially) to a fixed horizontal grounded metal plate kept at a specific electrode gap (d). The sample to be dried is kept directly above the grounded plate.[16] The needle electrode, also known as the Discharge electrode, is connected to a high-voltage AC or DC transformer (power supply). The high voltage output of the DC transformer can have either a positive or negative polarity. The transformer is connected to a voltage regulator to control the required high-voltage parameters for EHD drying. An electronically calibrated AC source supplies the voltage regulator's input. By adjusting the needle electrode's position along the vertical, the electrode gap can be changed to the required specification.[16,17] The drying rate increases with the increase in the applied voltage, but the voltage must be maintained to ensure that spark over doesn't occur. It has been observed from previous research that getting a higher drying rate requires having an ideal electrode gap and a sharp needle electrode.[18]

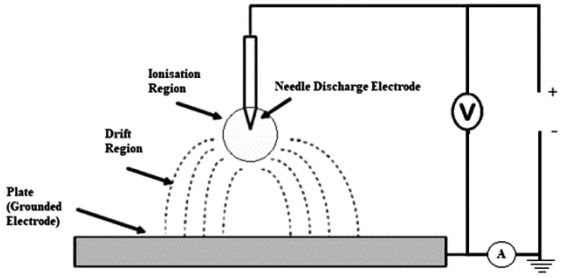

Fig. 1 — Corona discharge in a Point to plane configuration

The earliest found references to EHD go back to the seventeenth century[19] when William Gilbert's described how bringing a charged rod over a sessile drop causes a conical shape to form (Fig. 1). This conical shape formation is known as "Corona Discharge or Ionic Wind," it forms due to the difference in polarity between a charged electrode (discharge), a dielectric media (fluid), and a ground electrode (collector), as shown in Fig. 1. This corona discharge is essential for EHD drying applications, it is produced by charged gaseous ions that accelerate under the influence of a strong electric field. The corona discharge, which is also known as an ion-drag phenomenon, is caused when these charged ions collide with neutral molecules and transfer their momentum. EHD enhanced drying also depends on the corona discharge velocity (u_e), which results in the enhancement of mass transfer rates of the moisture within the sample.

This corona discharge influences the moist sample that is placed on the grounded plate or electrode, disrupting the saturated air layer and enhancing evaporation. As a result of this, the water molecules in the sample orient themselves toward the electric field, which causes the process's entropy to reduce. That lowers the temperature of the sample that is being dried.

In the theoretical study of the EHD enhanced drying problem, both the behaviour of a large number of ions in a dielectric medium and the behaviour of the sample in an electric field are taken into account. For a dielectric medium, Coulomb force or electrostatic force (F_e) forms the basis for volumetric electrostatic force (F), which is the force that acts on a unit volume of fluid, and it states that a force exists between two charged bodies in the presence of a fluid medium. The dielectric property of the fluid in an electrostatic field can be summed up by three forces[20] that are present during an EHD interaction and can be put into an equation as follows;

$$F = (\sigma E) - \left(\frac{\varepsilon_o}{2} E^2 \nabla \varepsilon\right) + \left[\frac{\varepsilon_o}{2} \nabla \left(E^2 \frac{d\varepsilon}{d\rho} \rho\right)\right] \quad \ldots(1)$$

Where, E is the electric field strength (kV/m), σ is the free charge density of ions ($1/m^3$), ε_o is dielectric

permittivity of vacuum (F/m), ρ is the mass density of air (kg/m^3), and ∇ is the vector gradient operator.

In Eq. 1, the first term defines the volumetric electrostatic force (F) (Coulomb's force), where the static force is related to the free electric charge present in the fluid. The second term defines the dielectric force; that is the non-uniformity of the dielectric constant 'ε' in a fluid volume that has been subjected to an electric field. And, the third term is the electrostrictive force, it is the force acting on a dielectric in a non-uniform electric field. The electrostrictive force is negligible if the fluid is incompressible ($\rho = const$).

Corona Discharge or Ionic Wind

Corona Discharge or Ionic Wind is the most significantly used term in EHD drying.[21] The transformation of electrical energy into mechanical energy causes the EHD phenomenon. When the mechanical energy causes the gas molecules to become ionized, the collision gives the molecules kinetic energy, which accelerates the molecules. As it can be seen in Fig. 1, the corona discharge is classified into 'the ionization-region, and 'the drift-region." The discharge electrode's tip is where avalanche ionisation occurs because of the acceleration of charged ions which collide with neutral gas molecules, this region is known as the ionisation region. When the gas molecules gain speed and move past the ionisation region, they create the drift region, which is bigger and mostly full of ions with the same polarity (positive or negative) as that of the discharge electrode.

The electric field gradually weakens after the ionisation region, and the charged ions lack the energy to ionise the gas molecules. As a result, avalanche ionisation ceases, and the amount of ions in the drift region gradually decreases. The electrohydrodynamic flow, also known as "corona wind or ionic wind," results from collisions between drifting charged ions and electrically neutral gas molecules in this region. The resulting ion flow velocity (u_e) can be evaluated by the expression (Eq. 2) derived from conservation of energy and Gauss law[22], which has been validated by Bashkir *et al.*;[23]

$$u_e = \frac{V}{d}\sqrt{\frac{\varepsilon_o}{\rho}} = E\sqrt{\frac{\varepsilon_o}{\rho}} \qquad \ldots(2)$$

Above equation (Eq. 2), was derived with an assumption that the electric field is uniform over the surfaces of grounded electrode but Henson[24] in his work had quoted that Warburg had discovered way back in 1889 that the discharge from the emitting electrode results in non-uniform distribution of electric current density (j) which generates a non-homogeneous electric field at the collector (ground) electrode surface as shown in Fig. 2. Robinson[25] extended this observation and derived a relation between corona discharge velocity (u_e) and the current density (j) over the surface of the grounded electrode, given by Eq. 3,

$$u_e = \sqrt{\frac{jd}{\rho b}} \qquad \ldots(3)$$

where, Current density (j) is given by Henson[24] and Jaworek & Krupa[26] as;

$$j = j_0 \cos^n \theta \qquad \ldots(4)$$

The 'n' values are 4.82 for positive discharge and 4.65 for negative discharge.[27,28] Instead, using 'n = 5' for both the polarities is sufficient for the majority of practical calculations.

Furthermore, Warburg[27] concluded that the cone angle (θ) should not exceed 60° for optimum performance of point to plane corona generator. The cone angle (θ), can be derived from Fig. 2, by taking into consideration the Radius of spread (R_c)

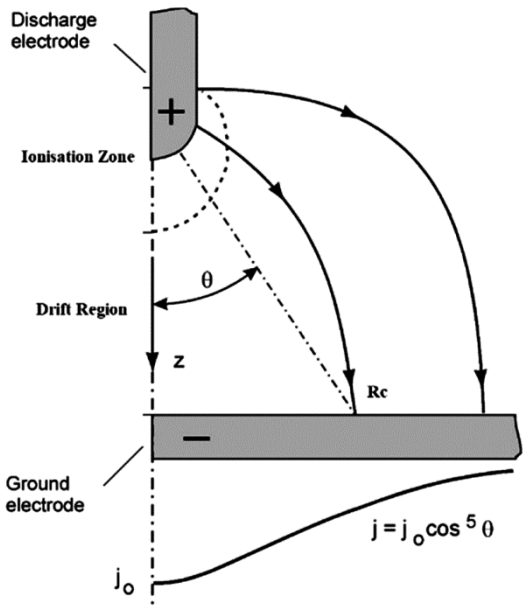

Fig. 2 — Warburg current density distribution

of the corona cone and the gap between the electrodes (d).

$$\theta = \tan^{-1}\left(\frac{R_c}{d}\right) \quad \ldots(5)$$

Hence, Eq. 3 further modifies to;

$$u_e = \sqrt{\frac{Id}{\rho A_p b}} \quad \ldots(6)$$

Where, I is Current (Amp), A_p is the area of collector (ground) electrode (m^2), and ' j ' is current per unit area.

Robinson[25] also observed that the discharge velocity calculated using Eq. 3 was much higher as compared to the one calculated using Eq. 6; he concluded that it must have been due to the initial assumption that there exists a uniform vertical gradient of the electric field strength between the discharge and collector electrodes. However, as per Warburg's Law, the distribution of current density along the horizontal planes between discharge and collector electrode (Eq. 3) would give the maximum discharge velocity (ionic wind), and Eq. 6 would give the average discharge velocity (ionic wind) over the cross-section of corona cone, which forms between the tip of discharge electrode and the ground electrode.

This discharge is generated between two electrodes, one of the electrodes is smaller in curvature as compared to the other, and both the electrodes are kept at opposite polarities. The smaller electrode is charged with a power supply resulting in ionization of surrounding gas (air) molecules, which are controlled by Coulomb force (F_e) (Eq. 7), and it results in the migration of ionized molecules towards the grounded electrode.

$$F_e = \frac{q_1 . q_2}{4\pi\varepsilon_0 S^2} = K_e \frac{q_1 . q_2}{S^2} \quad \ldots(7)$$

Where, F_e is Coulomb force, K_e is Coulomb Constant $8.987 \times 10^9 N.m^2 / C^2$, q_1, q_2 are the magnitudes of the charge on the two electrodes (C), and ' S ' is the distance between the two electrodes.

Current-Voltage (IV) Characteristics

The Current-Voltage characteristics (Fig. 3) enable us to better understand the various phases of corona discharge in the case of both Positive and Negative discharges, respectively.

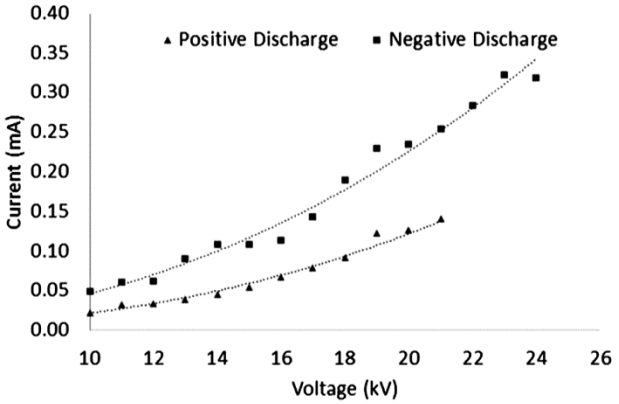

Fig. 3 — Current-Voltage (IV) Characteristic Curve for a fixed electrode gap

The discharge onset voltage (V_o) is the minimum voltage, which induces a current in the corona discharge. At this voltage, the ionization process at the tip of the discharge electrode starts, further increasing the voltage intensifies the ionization process. For voltages in the range of onset voltage (V_o), the corona current increases proportionally to the applied voltage (V).[29,30] A simple Townsend's equation (Eq. 8) gives the evolution of the current (I) as a function of applied voltage (V), irrespective of the applied potential. [27,31,29]

$$I = CV(V - V_o) \quad \ldots(8)$$

$$I = g\varepsilon_o b[V(V - V_0)] \quad \ldots(9)$$

Where, C is a constant depending upon the polarity of applied voltage, V_o is a function of the curvature of discharge needle electrode, g is the geometry parameter, ε_o is the dielectric permittivity of vacuum (8.85×10^{-12} F/m), and b stands for ionic mobility (m^2/Vs).

Henson[24] stated that Eq. 9 was derived for a uniform electric field, which is not a valid assumption, hence he modified Eq. 9 for a fully developed corona discharge, given by Eq. 10;

$$I = g\varepsilon_o b(V - V_0)^2 \quad \ldots(10)$$

The EHD drying parameter with the least amount of research is the geometry factor ' g '. This geometrical component is proportional to the area of the collecting electrode (A_p) and inversely

proportional to the gap (d), this observation is based on the results of earlier experiments.

Needle to Plane Electrode Configuration and Parameters Influencing the Drying Enhancement

A single needle-to-plane or point-to-plane corona discharge generator (Fig. 4), consists of a sharp-pointed electrically conducting needle-like electrode called the discharge electrode having a diameter (d_n). The discharge electrode is connected to a high voltage power source. The power source can be AC or DC, where a DC power source can be operated at either polarity (positive or negative), with an applied voltage (V) and current (I). A horizontal electrode that is electrically grounded, having a surface area of (A_p), is kept axially below the discharge electrode at a specific electrode gap (d), and it acts as the collector electrode. The drying sample is kept directly above this collector electrode, exposing it to the corona discharge emitting from the discharge electrode. Once the discharge electrode is supplied with current from the power source, and as the applied voltage reaches an onset value (V_o), the electrode starts emitting with a certain discharge velocity (u_e). This discharge or ionic wind results in the momentum of charged ions (positive or negative) between the two electrodes.

For a single-needle to plane electrode arrangement, the effectiveness of corona discharge in EHD drying enhancement can be evaluated by considering the influence of applied voltage (V) (positive or negative), electrode gap (d), electrode geometry, 'presence and absence' of cross-flow (u) (forced convection).

Effect of Polarity (Positive or Negative) on Drying Enhancement

Corona discharge occurs under both Positive and Negative applied potentials. Both of these discharge types have their effects on EHD enhanced drying.

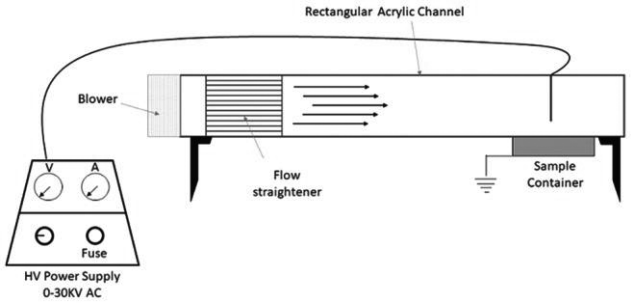

Fig. 4 — Experimental setup with single needle electrode configuration

These effects and characteristics have been discussed below.

Effects of Positive Corona Discharge

Positive corona discharge was found to give better drying enhancement and drying rate[32] because, in the case of negative corona discharge, a repulsive effect of ionized molecules exists between the emitting and ground electrode, which is having the same polarity.

While experimenting with a single needle to plane electrode arrangement, in a setup similar to the one shown in Fig. 4, Lai & Wong[16] and Alem-Rajabi & Lai[17] observed that the amount of specific energy consumed to evaporate one kilogram of water increased with the increase in applied voltage, and the best performance was achieved at a lower applied voltage. They also observed that the positive corona discharge had slightly better performance at lower applied voltage as compared to the negative corona discharge.

In their experiments Chen *et al.*[33] used drying samples of sliced potatoes with a sample thickness of 2, 4, and 8 mm, respectively. The sample was kept on the ground plate electrode and subjected to corona discharge emitting from the needle electrode at a positive applied potential of 5.25 kV at 3 mA current. They concluded that when the size of the potato slab is increased from 2 to 8 mm, the EHD drying system enhances the average rate of evaporation by a factor of 2.5 to 2.1 in comparison to the baseline values of the air-dried control samples of the same thickness. They concluded that the corona discharge generated due to the applied potential was the main driving force behind the enhancement in the drying of potato slabs.

Using a similar setup shown in Fig. 4, Barthakur & Arnold[34] evaluated the evaporation rate of water in a comparative study with ambient evaporation. They concluded that positive corona discharge results in a higher mass transfer coefficient, which was also evident in case of experiments conducted by Chen *et al.*[33], and a fact that was further validated by Barthakur[35] when he evaluated the drying rate of a saline sample and concluded that positive electric wind (corona discharge) was principle driving force behind rapid drying rate of the saline solution.

One of the significant observations was regarding the polarity of applied potential and its impact on drying rate; Barthakur & Kanani[36] concluded that the positive discharge produced by the corona generator was more than the negative discharge, indicating that

positive ions are more effective in increasing the drying rate of liquid as compared to the negative one.

Effects of Negative Corona Discharge

For a single needle-to-plane electrode configuration, the effects of negative corona discharge on drying enhancement have been studied by very few researchers. The primary reason for it is that the negative corona discharge experiences a suppressing effect, which is due to the similar polarity of both the discharge ions and the ground electrode. It reduces the effectivity of the negative corona discharge on overall drying enhancement in an EHD drying application. Alem-Rajabi & Lai[17] observed that because of this suppressing effect, the drying rate achieved by negative corona discharges was lesser as compared to the one in the case of positive corona discharge. Similar observations were quoted by Lai & Wong.[16]

Defoort *et al.*[37] validated this suppressing effect, when they tried to establish, and ascertain laws of 'Electrohydrodynamic phenomenon' by considering an experimental setup which was having a fixed electrode gap (d) of 15mm. They were also able to re-establish the fact that the *IV* characteristic curve of negative discharge justified Townsend's law (Eq.8). Similarly, the negative corona discharge results in constant ionic wind velocity between the electrodes, even in the presence of the Trichel pulse, and the velocity is maximum at the tip of the electrode. It goes on reducing as it approached the ground, an observation that has been quoted by Moreau *et al.*[29] and Lama & Gallo[38] as well.

Moreau et al.[29] investigated the flow characteristics of negative corona discharge and observed that as compared to the positive corona discharge, the discharge flow rate (u_e) was far lesser at the same applied potential. Negative corona discharge results in drying enhancement, yet due to the lower discharge flow rate (u_e) and the suppressing effect overall drying rate remains low.

Lai & Wong[16] observed that the negative corona discharge results in turbulence, which effectively benefits the EHD drying enhancement. However, at the same time, it consumes more power as compared to positive corona discharge resulting in inferior performance in terms of energy consumption. Moreover, the rate of drying enhancement was relatively slower as compared to the positive corona discharge even in the presence of a cross-flow.

The drying rate was thus related to the rate of increase in the applied voltage for both positive and negative corona discharges,[33,39] indicating that the drying rate may be successfully regulated by adjusting the applied voltage within the inception and breakdown voltage.

Effects of Geometry and Electrode Gap

Geometric Parameters of discharge electrode, like electrode gap (d) and electrode needle tip curvature are two significant parameters that have influenced the EHD drying enhancement process in the case of a single-needle to plane electrode EHD drying applications.[40] These parameters have been known to influence the corona discharge behaviour, thus affecting its effectiveness in drying enhancement. Similarly, these parameters have been known to affect the energy utilization aspect of an EHD process as well.[10,41]

Hashinaga *et al.*[42] had used two types of needle electrodes in their experimentation, a thin sewing needle with a fine point and a thick needle with a blunt point. They observed that the effectiveness of the thinner needle in drying enhancement was more profound as compared to the thicker needle (Fig. 5), indicating that needle geometry and tip curvature both have a significant role to play in EHD drying enhancement. Similarly, the drying rate was seen to be influenced by the electrode gap (d) as well (Fig. 5), wherein an electrode gap of 15 mm was showing the maximum effectiveness for the thinner sewing needle electrode.

The effect of needle electrode geometry on corona discharge was first reported by Precht.[43], he experimented with a conical electrode with tip angles varying from 15 to 90°; he reported that the sharper

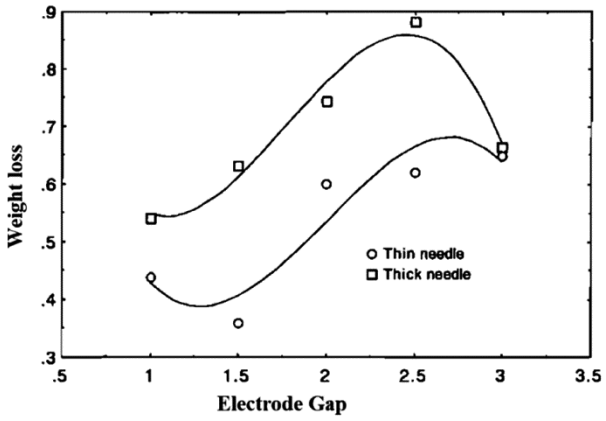

Fig. 5 — EHD drying as a function of electrode gap (d) and the type of the discharge Electrodes

electrode requires a lower voltage to initiate corona discharge. Thus, the same voltage results in a higher discharge current from the sharper electrode (smallest tip angle).

Lama *et al.*[38] were amongst the first to study the effect of needle tip radius of the discharge electrode on the behavior of Trichel pulse in a corona discharge. They concluded that irrespective of the tip diameter of the discharge electrode, as long as the needle is thin and the tip diameter is smaller than the electrode gap (d), there would be a proportionality between current (I) and applied voltage (V). The distortion in the corona was visible only near the tip of the discharge needle for various needle diameters and hence was a localized phenomenon. With the progression (as we go away from the tip along the vertical axis towards the ground electrode), this distortion had a negligible effect on the flow behaviour of corona discharge.

Using a point-to-plane configuration Kip[10] studied the variation in IV characteristics in a positive discharge. As can be seen from Fig. 6, as the electrode gap increases, there is a fall in initial current, which was attributed to the change in electric field distribution between the electrodes (discharge and ground/collector). Moreover, this observation was also validated by Barthakur & Arnold[34] and Kip[10], both experimentally and numerically. They noted that the current distribution density is affected significantly by the electrode gap (d), as has been predicted by Henson.[24]

To study the field strength distribution along the needle axis between the discharge tip and collector electrode ($d = 40mm$), Altamimi *et al.*[40] experimented with three types of discharge electrodes; sharp, flat, and spherical. They noticed that the shape of the discharge electrode had a considerable impact on the characteristics of corona discharge and distribution strength of the electric fields, the sharp needle showing the most uniform electric field distribution (Fig. 7). These results indicated that electric field magnitude is highest at the tip of the sharp needle as compared to the flat or spherical tip. A higher electric field magnitude results in more ionizations, resulting in a more extended streamer formation during corona discharge at a low corona inception voltage(V_o). Hence, a better drying rate is achieved in EHD-driven applications.

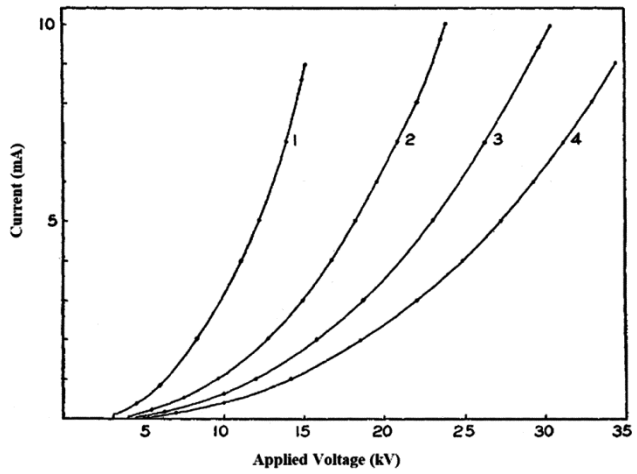

Fig. 6 — IV characteristics with variable electrode gap

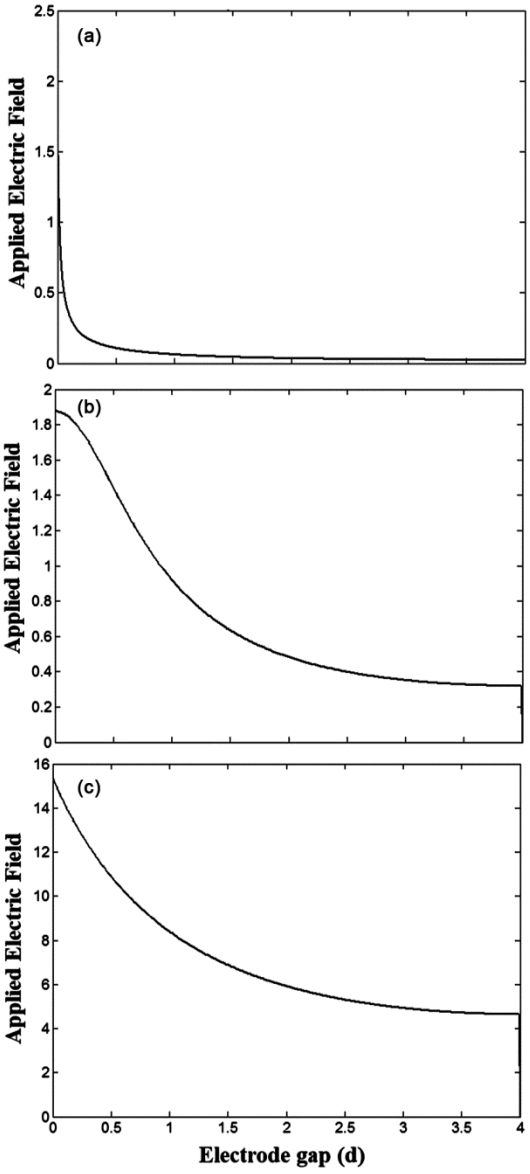

Fig. 7 — Electric field strength distribution for different types of electrodes: (a) Sharp, (b) Flat, and (c) Sphere

Kip[10] also observed that for an 'electrode gap (d)' to 'needle tip radius (r)' ratio (d/r), a larger value would result in lower current values since the discharge relaxation time is more and would result in a weak discharge sweeping field over the collector. With a smaller electrode gap, the sweeping field would be more uniform, and current stability would be higher. Ahmedou *et al.*[44] and Lai & Wong[16] concluded that further reducing the electrode gap would result in early breakdown and spark over at a smaller applied voltage. Hence, an optimum combination of electrode gap (d) and discharge tip radius (r) would yield the desired outcome for a given EHD drying application.

Whereas, when it came to evaluating the effectiveness of the discharge gap on EHD-driven applications Chen & Barthakur[39], Barthakur & Arnold[34] and Lai & Wong[16] experimented with an electrode gap of 5,10, and 20 mm. It was observed that for an electrode gap of 10 mm, the effectiveness of drying was most significant in the case of both positive and negative corona discharge, indicating a possible optimum electrode gap for stable corona discharge, as has been discussed by Kip[10] earlier. It was also observed that for an electrode gap of 5 mm, the current drawn(μA) was much higher as compared to the other two electrode gaps, even though the ion flow velocity (m/s) was higher, yet the power consumption had significantly increased. Similar observations were made by Lai & Wong[16], wherein they experimented with two electrode gaps of 12.7 mm and 25.4 mm to enhance the drying of glass beads saturated with water. They observed that for an electrode gap of 12.7 mm, the performance of the EHD drying mechanism was much better both in terms of power consumption and drying effectiveness.

Thus, it can be said that the geometry of the electrode significantly affects both the behavior of corona discharge and the enhancement of drying. With an optimum electrode gap (d) one could induce stable corona discharge.[10] And an optimum 'electrode gap (d)' to 'needle tip radius (r)' ratio (d/r) would result in the enhancement of the drying process with minimal power consumption.[10]

On the contrary, one of the geometric parameters, the needle diameter, was found to have no significant effect on drying rate enhancement[45], rather it was the needle tip type that was found to be the one that determined the distribution of corona cone. Where, in comparison to a flat or a hemispherical needle tip, a needle with a finer tip (conical) gives more uniform corona discharge distribution, and hence it is more efficient in increasing drying rate.[42,45]

Effects of Cross-Flow on EHD Enhancement

The effect of cross-flow (forced convection) on the effectiveness of corona discharge in an EHD drying mechanism has been studied by many. Lai & Sharma[9] and Dalvand *et al.*[46,47] found that cross-flow can severely affect the efficiency of the drying mechanism. Depending upon the velocity of cross-flow[48], higher flow velocities were found to suppress the corona discharge rendering it ineffective in drying enhancement. Huang & Lai[49] stated that, at the same time, lower velocity cross-flow had been reported to assist in the EHD drying process; and it would yield a drying rate better than the one achieved in the absence of cross-flow.

Berendt *et al.*[50] used a setup similar in appearance to the one shown in Fig. 4, to assess the efficiency of negative corona discharge and its electrical properties when a cross-flow is present. They also concluded that negative corona discharge is generally suppressed by cross-flow, whether transverse or longitudinal over the sample surface. To govern the effectiveness and utility of cross-flow, researchers proposed a dimensionless EHD number (N_{EHD}) (Eq. 11), defined as the ratio of Ion-flow velocity or corona discharge velocity (u_e) and cross-flow velocity (forced convection) (u);

$$N_{EHD} = \frac{u_e}{u} \qquad \ldots(11)$$

Low cross-flow velocity creates favorable circumstances for convective mass transfer with minimal corona discharge distortion (ionic wind). Lai & Sharma[9] and Rezaee *et al.*[51] in their studies used dimensionless numbers to investigate the effect of corona wind on convective mass transfer.

A setup similar to the one shown in Fig. 4, has been used by many researchers for this evaluation. Alem-Rajabi & Lai[17] studied the effect of cross-flow (forced convection) on EHD drying; they expressed it using an arbitrary EHD number (N_{EHD}). They observed that if this EHD number ($N_{EHD} > 1$), the effect of drying enhancement was significant, and for ($N_{EHD} < 1$), they observed a considerable reduction in drying rate. This EHD number is equivalent to the square root of the force ratio (Ion-drag force/ inertial

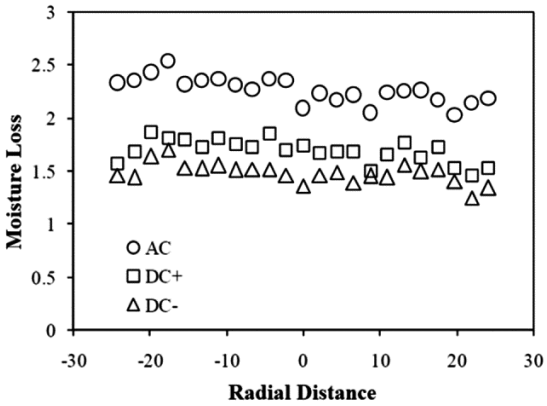

Fig. 8 — Effect of polarity on water evaporation rate

force).[52] They had experimented with variable cross-flow velocities and observed that it assists in drying enhancement, but its effectiveness becomes insignificant as the water level in the sample container starts reducing. They also concluded that at lower cross-flow velocity ($u \leq 0.7 - m/s$), the rate of drying enhancement was non-linear, but for higher velocities ($u \geq 1.0 - m/s$), it becomes linear. A similar observation was made by Lai *et al.*[48], that the evaporation rate was lower in the presence of large cross-flow as it tends to suppress the corona wind, affecting the drying enhancement significantly, whereas the drying rate increased linearly in the absence of cross-flow.

To summarize the effect of cross-flow velocity (forced convection), a low velocity was found to assist in drying enhancement as it does not suppress the corona discharge, and it would also contribute to the evaporative drying process; for ($N_{EHD} > 1$), the effect of EHD drying enhancement was found to be significant as compared to the one with ($N_{EHD} < 1$).[17,48] And a low cross-flow velocity with higher voltage discharge resulted in higher drying rates as compared to the one in the absence of cross-flow (forced convection).[53]

Effects of AC and DC Applied Voltage

Direct current (DC) or alternating current (AC) can both cause corona discharge in EHD drying applications. The polarity of the applied voltage determines whether the DC corona discharge is positive or negative. In comparison, the applied voltage in an AC corona discharge changes polarity with each cycle, leading to a discontinuous discharge. But the performance efficiency of AC corona discharge-driven EHD drying applications is more than the DC corona discharge[45–54] (Fig. 8).

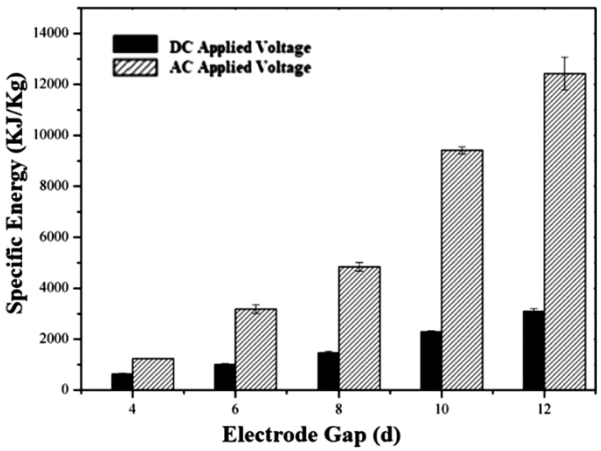

Fig. 9 — Specific Energy Consumption as a function of the electrode gap

Hashinaga *et al.*[42] validated that AC applied voltage had the potential to enhance the water evaporation rate, and the electrode gap (d) has a critical role to play in the enhancement process. Yang & Ding[54] observed that the drying rate increase with the increase in applied voltage, an observation which has been quoted by many for both AC and DC applied voltages. Ding *et al.*[55] reported that irrespective of applied field intensity, the thickness of the drying sample would retard the drying rate, reducing overall drying efficiency.

Yang *et al.*[56] while experimenting with variable discharge gap (d), for similar operating conditions of AC and DC corona discharges, respectively, found that the drying rate in the case of both AC and DC applied potential was pretty much the same, but the specific energy consumption (Fig. 9) in the case of AC applied potential was much higher as compared to the DC for all the discharge gaps (d). They concluded that an appropriate combination of DC applied voltage and electrode gap would result in a high drying rate with lesser energy consumption.

AC corona discharge was found to be more effective in drying enhancement, (Fig. 8) as compared to both positive and negative DC corona discharge.[45–54] However, AC corona discharge consumes significantly more energy (Fig. 9) due to the fluctuating nature which results in discontinuous discharge, thus affecting the overall power consumption.[56]

Conclusions

In this paper, the effectiveness of corona discharge under various performance parameters, for a needle to plane electrode configuration and its role in EHD

drying enhancement have been discussed. For effective EHD drying enhancement, parameters like applied voltage (AC or DC), polarity (positive or negative), type of needle, electrode geometry, electrode gap (d), and cross-flow velocity (forced convection) were discussed for their role in generating efficient corona discharge. These parameters have their individual effects that have been studied by various researchers, yet a large-scale application for commercial drying or industrial implementation has not yet been developed.

An optimized model based upon the above parameters and the observations needs to be investigated thoroughly for the development of the needle-to-plane EHD drying model for industrial application, as it might be able to address the challenges associated with the upscaling of the model. And it can also provide a solution for addressing the non-uniform drying and inefficient mass drying problems, which are associated with the upscaling of experimental models to suit the volume of industrial needs.

References

1 Bai Y X & Sun B, Study of electrohydrodynamic (EHD) drying technique for shrimps, *J Food Process Preserv*, **35(6)** (2011) 891–897.

2 Esehaghbeygi A, Pirnazari K & Sadeghi M, Quality assessment of electrohydrodynamic and microwave dehydrated banana slices, *LWT - Food Sci Technol,* **55(2) (**2014) 565–571.

3 Li F D, Li L T, Sun J F & Tatsumi E, Effect of electrohydrodynamic (EHD) technique on drying process and appearance of okara cake, *J Food Eng,* **77(2)** (2006) 275–280.

4 Alemrajabi A A, Rezaee F, Mirhosseini M & Esehaghbeygi A, Comparative evaluation of the effects of electrohydrodynamic, oven, and ambient air on carrot cylindrical slices during drying process, *Dry Technol,* **30(1)** (2012) 88–96.

5 Ratti C, Hot air and freeze-drying of high-value foods: A review, *J Food Eng,* **49(4) (**2001) 311–319.

6 Lai F C & Wang C C, Drying of partially wetted materials with corona wind and auxiliary heat, *Proc ESA Annual Meeting on Electrostatics Paper B1* (Electrostatic Society of America, Minneapolis) 2008.

7 Amami E, Vorobiev E & Kechaou N, Effect of pulsed electric field on the osmotic dehydration and mass transfer kinetics of apple tissue, *Dry Technol*, **23(3)** (2005) 581–595.

8 Bai Y X, Yang G J, Hu Y C & Qu M, Physical and sensory properties of electrohydrodynamic (EHD) dried scallop muscle, *J Aquat Food Prod Technol,* **1(3)** (2012) 238–247.

9 Lai F C & Sharma R K, EHD-enhanced drying with multiple needle electrode, *J Electrostat,* **63(3-4)** (2005) 223–237.

10 Kip A F, Positive-point-to-plane discharge in air at atmospheric pressure, *Phys Rev*, **54(2) (**1938) 39–146.

11 Khalifa M M & Morris R M, A Laboratory Study of the Effects of Wind on DC Corona, *IEEE Trans Power Appar Syst*, **86(3) (**1967) 290–298.

12 Morrison R D & Hopstock D M, The distribution of current in wire-to-cylinder corona, *J Electrostat*, **6(4) (**1979) 49–360.

13 Zhang Y, Liu L, Chen Y & Ouyang J, Characteristics of ionic wind in needle-to-ring corona discharge, *J Electrostat*, **74** (2015) 15–20.

14 Defraeye T & Martynenko A, What Is Preventing Electrohydrodynamic Drying Technology From Being Applied Industrially, And What Can We Do About It?, *Sci trends*, 26, October 2018.

15 Singh A, Orsat V & Raghavan V A, Comprehensive Review on Electrohydrodynamic Drying and High-Voltage Electric Field in the Context of Food and Bioprocessing, *Dry Technol*, **30(16)** (2012) 1812–1820.

16 Lai F C & Wong D S, EHD-enhanced drying with needle electrode, *Dry Technol,* **21(7) (**2003) 1291–1306.

17 Alem-Rajabi A & Lai F C, EHD-enhanced drying of partially wetted glass beads, *Dry Technol,* **23(3) (**2005) 597–609.

18 Bajgai T R, Raghavan G S V, Hashinaga F & Ngadi M O, Electrohydrodynamic drying - A concise overview, *Dry Technol*, **24(7) (**2006) 905–910.

19 Saville D A, ELECTROHYDRODYNAMICS: The Taylor-Melcher Leaky Dielectric Model, *Annu Rev Fluid Mech*, **29(1)** (1997) 27–64.

20 Panofsky W K H, Phillips M & Dwight C H, Classical Electricity and Magnetism, *Am J Phys* **31(3) (**1963) 224–224.

21 Kudra T & Martynenko A, Electrohydrodynamic drying: Theory and experimental validation, *Dry Technol*, **38(1-2)** (2020) 168–175.

22 Cross J, Electrostatically assisted heat transfer, *Electrostatistics Inst Phys,* **48 (**1979) 191–199.

23 Bashkir I, Defraeye T, Kudra T & Martynenko A, Electrohydrodynamic Drying of Plant-Based Foods and Food Model Systems, *Food Eng Rev*, **12(14)** (2020) 473–497.

24 Henson B L, A derivation of Warburg's law for point to plane coronas, *J Appl Phys*, **52(6) (**1981) 3921–3923.

25 Robinson M, Movement of air in the electric wind of the corona discharge, *Trans AIEE*, **80(2) (**2013) 143–150.

26 Jaworek A & Krupa A, Electrical characteristics of a corona discharge reactor of multipoint-to-plane geometry, *Czechoslov J Phys,* **45(12)** (1995) 1035–1047.

27 Warburg E, About discharge from sharp pin, *Wiedermann Annalen,* **67 (**1899) 69–83.

28 Dalvi-Isfahan M, Hamdami N, Le-Bail A & Xanthakis E, The Principles of High Voltage Electric Field and Its Application in Food Processing: A Review, F*ood Res Int*, **(89)** (2016) 48–62.

29 Moreau E, Audier P & Benard N, Ionic wind produced by positive and negative corona discharges in air, *J Electrostat*, **93** (2018) 85–96.

30 Martynenko A, Astatkie T & Defraeye T, The role of convection in electrohydrodynamic drying, *J Food Eng*, **271** (2020) 109777.

31 Zeleny J, Physical review, *J J phys theor appl*, **7(1)** (1898) 161–167.

32 Barthakur N N & Al-kanani T, A comparative study between an electrostatic and conventional methods of drying soil samples, *Commun Soil Sci Plant Anal*, **20(13-14)** (1989) 1261–1277.

33 Chen Y, Barthakur N N & Arnold N P. Electrohydrodynamic (EHD) drying of potato slabs. *J Food Eng.* **23(1)** (1994) 107–119.

34 Barthakur N N & Arnold N P, Evaporation rate enhancement of water with air ions from a corona discharge, *Int J Biometeorol*, **39(1)** (1995) 29–33.

35 Barthakur N N, An electrostatic method of drying saline water, *Dry Technol*, **7(3)** (1989) 503–521.

36 Barthakur N N & T Al-Kanani, Impact of air ions of both polarity on evaporation of certain organic and inorganic liquids, *Int J Biometeorol*, **33(2)** (1989) 136–141.

37 Defoort E, Bellanger R, Batiot-Dupeyrat C & Moreau E, Ionic wind produced by a DC needle-to-plate corona discharge with a gap of 15 mm, *J Phys D Appl Phys*, **53(17)** (2020) 175202.

38 Lama W L & Gallo C F, Systematic study of the electrical characteristics of the "trichel" current pulses from negative needle-to-plane coronas, *J Appl Phys*, **45(1)** (1974) 103–113.

39 Chen Y H & Barthakur N N, Potato slab dehydration by air ions from corona discharge, *Int J Biometeorol*, **35(2)** (1991) 67–70.

40 Altamimi G, Illias H A, Mokhtar N, Mokhlis H & Bakar A H A, Corona discharges under various types of electrodes, *IEEE Int Conf on Power and Energy*, (2014) 5–8.

41 Martynenko A & Kudra T, Electrohydrodynamic dryer: Effect of emitters' density and gap between discharge and collecting electrodes, *Dry Technol*, **38(1-2)** (2020) 158–167.

42 Hashinaga F, Bajgai T R, Isobe S & Barthakur N N, Electrohydrodynamic (EHD) drying of apple slices, *Dry Technol*, **17(3) (**1999) 479–495.

43 Precht J, Absolute measurements of electric discharge from pointed rods, *Ann Phys*, **285(5)** (1893) 150–183.

44 Ould Ahmedou S A, Rouaud O & Havet M, Electrohydrodynamic enhancement of heat and mass transfer in food processes, in *3rd International Symposium on Food and Agricultural Products* (Naples Italy) 24–26 September 2007.

45 Zheng D J, Liu H J, Cheng Y Q & Li L Te, Electrode configuration and polarity effects on water evaporation enhancement by electric field, *Int J Food Eng*, **7(2)** (2011).

46 Dalvand M J, Mohtasebi S S & Rafiee S, Modeling of electrohydrodynamic drying process using response surface methodology, *Food Sci Nutr*, **2(3)** (2014) 200–209.

47 Dalvand M J, Mohtasebi S S & Rafiee S, Optimization on drying conditions of a solar electrohydrodynamic drying system based on desirability concept, *Food Sci Nutr*, **2(6)** (2014) 758–767.

48 Lai F C, Huang M & Wong D S, EHD-enhanced water evaporation, *Dry Technol*, **22(3)** (2004) 597–608.

49 Huang M & Lai F C, Numerical study of EHD-enhanced water evaporation, *J Electrostat*, **68(4)** (2010) 364–370.

50 Berendt A, Budnarowska M & Mizeraczyk J, DC negative corona discharge characteristics in air flowing transversely and longitudinally through a needle-plate electrode gap, *J Electrostat*, **92** (2018) 24–30.

51 Rezaee F, Esehaghbeygi A, Mirhosseini M & Alemrajabi A A, Electrohydrodynamic drying of kiwi (Actinidia chinensis) slices, *Agric Eng Int: CIGR J*, **22(4)** (2020) 221–228.

52 Sadek S E, Fax R G & Hurwitz M, The influence of electric fields on convective heat and mass transfer from a horizontal surface under forced convection, *J Heat Transfer*, **94(2)** (1972) 144–148.

53 Martynenko A, Bashkir I & Kudra T,, Electrically enhanced drying of white champignons, *Dry Technol*, **39(2)** (2021) 234–244.

54 Yang M & Ding C, Electrohydrodynamic (EHD) drying of the Chinese wolfberry fruits, *SpringerPlus*, **5(1)** (2016) 1–20.

55 Ding C, Lu J, Song Z & Bao S, The drying efficiency of electrohydrodynamic (EHD) systems based on the drying characteristics of cooked beef and mathematical modeling, *Int J Appl Electromagn*, **46(3)** (2014) 455–461.

56 Yang M, Ding C & Zhu J, The drying quality and energy consumption of Chinese wolfberry fruits under electrohydrodynamic system, *Int J Appl Electromagn*, **55(1)** (2017) 01–112.